euronoise

On the adsorption-desorption relaxation time of carbon in very narrow ducts

Timothy Mellow[a], Olga Umnova[b], Konstantinos Drossos[c], Keith Holland[c], Andrew Flewitt[d] and Leo Kärkkäinen[e]

[a]Nokia, Nokia House, Summit Avenue, GU14 0NG Farnborough, UK
[b]University of Salford, Acoustics Research Centre, Newton Building, M5 4WT Salford, UK
[c]University of Southampton: Institute of Sound and Vibration Research, University Road, Highfield, SO17 1BJ Southampton, UK
[d]University of Cambridge: Centre for Advanced Photonics and Electronics, 9, JJ Thomson Ave., CB3 0FA Cambridge, UK
[e]Nokia Research Center, Itämerenkatu 11 - 13, 00180 Helsinki, Finland
tim.mellow@nokia.com

Loudspeakers generally have boxes to prevent rear wave cancellation at low frequencies. However, the stiffness of the air in a small box reduces the diaphragm's excursion at low frequencies. Hence the box size is generally a compromise between low frequency performance and practicality. Activated carbon has been found to increase the apparent size of a given box through adsorption of the air molecules when the pressure increases and likewise desorption when it decreases. However, the exact viscous effects in the granular structure are difficult to model. Thus it is impossible determine the high frequency limit due to the natural adsorption/desorption relaxation time in the absence of viscous losses.

In this study, a tube model is presented which takes into account viscous and thermal losses with boundary slip together with adsorption. Impedance measurements are performed on an array of 12 million holes, each 2 micrometers in diameter, etched in a 0.25 mm thick silicon wafer so that the viscous and thermal losses can be verified against the model without adsorption. Impedance measurements are then performed on an array of holes coated with graphite in order to create an activated carbon-like structure, thus enabling the adsorption/desorption relaxation time to be evaluated.

1 Introduction

In recent years, activated carbon has been used to reduce the size of hi-fi loudspeaker cabinets [1] and has been studied theoretically by Bechwati *et. al.*.[2] It works by adsorbing air molecules when there is an increase in pressure and then releasing them again when the pressure falls. This reduces the net stiffness due to the air trapped in the cabinet and enables the loudspeaker diaphragm to move more freely at low frequencies. The net effect of this is to lower the fundamental resonant frequency, thus boosting the bass response of the loudspeaker. Alternatively, the cabinet size can be reduced without changing the resonant frequency. However, evidence so far suggests that the effect decreases rapidly above 150 Hz, thus rendering it unsuitable for mobile applications, where the fundamental resonance of the loudspeaker is typically in the range 700-1000 Hz. Two effects determine this upper frequency limit. One is the natural adsorption/desorption relaxation time of the carbon itself and the other is the resistance due to viscous losses. The latter is a property of the structure of the material and the geometry of the path which the air has to take in order to reach the micro-pores.

The purpose of this study is to create a model of a structure with a much simpler structure than typical granular activated carbon, namely a parallel array of micro-tubes etched in silicon and lined with graphite, which can then be measured in order to determine the unknown parameters such as the adsorption/desorption relaxation time and adsorption capacity. This is made possible by the fact that the other parameters, such as the viscous and thermal losses can be determined in advance using known equations [3] for a circular tube of radius a and length h with significant boundary slip. A lumped parameter model is developed for the tube together with formulas for the circuit elements. Veijola [4] reported similar formulas for a T-network model of a microchannel without adsorption, although the topology of the thermal conduction elements was slightly different. Specific impedance is used throughout, which is the ratio of the driving pressure to particle velocity at the mouth, so that the specific acoustic impedance of a single tube is the same as that of an array, except for a fill-factor which is the ratio of the total area of the tube entrances to the total area of the wall which they partially occupy.

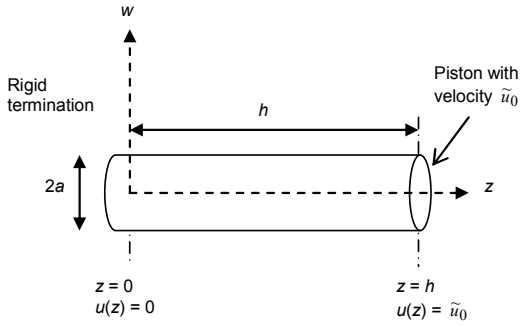

Figure 1. Geometry of the tube model.

2 Assumptions

Each duct is modelled as a circular tube with a rigid end termination as shown in Figure 1, with z as the axial ordinate and w as the radial ordinate. The aspect ratio is such that end corrections are neglected. In the following discussion, it is assumed that the radial pressure distribution is constant and the pressure variations are purely axial. Also, it is assumed that the radial velocity is zero, but the axial velocity is allowed to vary radially due to laminar flow resulting from viscous losses. Thermal conduction through the tube wall is also taken into consideration. However, boundary slip is allowed for, whereby the axial velocity at the tube wall can be non-zero and the temperature there can be non-ambient. Finally, a model for air molecule adsorption and desorption resulting from the pressure fluctuations is included. Although adsorption will only occur at the tube wall, it is assumed that the air molecules are mobile enough for this to be treated as "bulk" adsorption throughout the tube. Considering that the average speed of an air molecule at room temperature is around 500 m/s, this seems a reasonable assumption.

3 Wave equation for an infinite tube with adsorption

3.1 Adsorption equation

The adsorption dynamics equation is

$$\frac{dn_a}{dt} = k_a P(N - n_a) - k_d n_a, \qquad (1)$$

where P is the pressure in the ducts, n_a is the number of adsorbed molecules per unit surface area, k_a is the adsorption coefficient in $\mathrm{Pa^{-1}s^{-1}}$, and k_d is the desorption coefficient in $\mathrm{s^{-1}}$. N is the maximum number of adsorbed

molecules per unit surface area. The coefficients k_a and k_d are defined by

$$k_a = \frac{c_a}{\sqrt{2\pi mkT_0}} e^{-E_a/(RT_0)} \qquad (2)$$

and

$$k_d = c_d e^{-E_d/(RT_0)} \qquad (3)$$

respectively where c_a and c_d are constants, $m = 4.81 \times 10^{-26}$ kg is the mass of an air molecule, k is Boltzmann's constant, R is the ideal gas constant, $T_0 = 295$ K is the static temperature, and E_a and E_d are the activation energies of adsorption and desorption respectively. Although k_a and k_d are dependent upon temperature, they will be assumed to be constants for the purpose of this study. At equilibrium, where $\frac{dn_a}{dt} = 0$, this leads to the Langmuir adsorption isotherm:

$$n_a^e = \frac{k_a P_0 N}{k_a P_0 + k_d}, \qquad (4)$$

where n_a^e is the number of adsorbed molecules at equilibrium and $P_0 = 10^5$ N/m^2 is the static pressure. We now redefine n_a, n_a^e and N as densities ρ_a, ρ_a^e and ρ_N respectively so that Eqs. (1) and (4) can be rewritten as

$$\frac{d\rho_a}{dt} = k_a P(\rho_N - \rho_a) - k_d \rho_a, \qquad (5)$$

$$\rho_a^e = \frac{k_a P_0 \rho_N}{k_a P_0 + k_d}. \qquad (6)$$

In order to define ρ_N, let a volume element of the tube be expressed as $\Delta V = \pi a^2 \Delta h$, where a is the radius of the tube and Δh is the elemental length. Let n be the maximum number of molecules that can be adsorbed over the internal surface of the volume element as defined by $n = 2\pi Na\Delta h$. The maximum adsorbed density ρ_N and adsorbed density ρ_a are then $\rho_N = nm/(\Delta V) = 2Nm/a = 2\sigma/a$, $\rho_a = 2n_a m/a = 2n_a\sigma/(Na)$ respectively, where $\sigma = Nm = m/S_m$ is the surface mass density that can be accommodated, where S_m is the area occupied by each air molecule, which is assumed to be 1.3×10^{-20} m^2. Thus it can be seen that reducing the size and increasing the number of tubes increases the amount of air that can be adsorbed. We can linearize Eq. (5) by letting $P = P_0 + p$ and $\rho_a = \rho_a^e + \delta_a$ as follows:

$$\frac{d\delta_a}{dt} \approx \frac{k_a k_d \rho_N}{\omega_a} p - \omega_a \delta_a, \qquad (7)$$

where ω_a is the adsorption-desorption cut-off frequency or inverse of the adsorption-desorption relaxation time given by

$$\omega_a = k_a P_0 + k_d. \qquad (8)$$

Replacing the time derivative with $i\omega$ gives

$$\tilde{\delta}_a = \frac{k_a k_d \rho_N}{(i\omega + \omega_a)\omega_a} \tilde{p}. \qquad (9)$$

where the tilde denotes a harmonically varying parameter after omitting the factor of $e^{i\omega t}$.

3.2 Momentum conservation equation

In accordance with the conservation of momentum law, we can write the linearized Navier-Stokes equation [5]

$$\left(\rho_0 \frac{\partial}{\partial t} - \mu\nabla^2\right) u(w) = -\frac{\partial p}{\partial z}, \qquad (10)$$

where $\nabla^2 = \partial^2/(\partial w^2) + w^{-1}\partial/(\partial w)$ and u is the axial velocity, p is the axial pressure, $\rho_0 = 1.18$ kg/m^3 and $\mu = 17.8 \times 10^{-6}$ Ns/m^2 are the density and viscosity of air respectively, and z is the axial ordinate. Replacing the time derivative with $i\omega$ gives

$$(\nabla^2 + k_V^2)\tilde{u}(w) = -\frac{k_V^2}{i\omega\rho_0}\frac{\partial \tilde{p}}{\partial z}, \qquad (11)$$

where $k_V = \sqrt{-i\omega\rho_0/\mu}$.

3.3 Gas law and thermal conduction (entropy)

For an ideal gas [5]

$$\tilde{p}/P_0 = \tilde{\delta}/\rho_0 + \tilde{\tau}(w)/T_0, \qquad (12)$$

where $\tilde{p}$, $\tilde{\delta}$ and $\tilde{\tau}$ are the small pressure, density and temperature fluctuations respectively. The equation for thermal conduction is

$$\kappa\nabla^2\tilde{\tau}(w) = i\omega T_0(\rho_0 C_V \tilde{p}/P_0 - C_P\tilde{\delta}), \qquad (13)$$

where $\kappa = 25.4 \times 10^{-3}$ N/s/K is the thermal conductivity. Eliminating $\tilde{\delta}$ from Eqs. (12) and (13) gives

$$\kappa\nabla^2\tilde{\tau}(w) = i\omega\rho_0 T_0\left((C_V - C_P)\frac{\tilde{p}}{P_0} + C_P\frac{\tilde{\tau}(w)}{T_0}\right). \qquad (14)$$

We also note that $C_P - C_V = P_0/(\rho_0 T_0)$ so that

$$(\nabla^2 + P_r k_V^2)\tilde{\tau}(w) = \frac{P_r k_V^2}{\rho_0 C_P}\tilde{p}, \qquad (15)$$

where the P_r is the (dimensionless) Prandtl number given by $P_r = \mu C_P/\kappa$.

3.4 Solution of the velocity and temperature radial equations

Equations (11) and (15) for the radial velocity and temperature distributions respectively are subject to the following slip boundary conditions

$$\tilde{u}_a = -aB_u \left.\frac{\partial\tilde{u}(w)}{\partial w}\right|_{w=a}, \qquad (16)$$

$$\tilde{\tau}_a = -aB_e \left.\frac{\partial\tilde{\tau}(w)}{\partial w}\right|_{w=a}, \qquad (17)$$

where the boundary slip factors B_u and B_e are given by $B_u = (2\alpha_u^{-1} - 1)K_n$, $B_e = (2\gamma/P_r(1+\gamma))(2\alpha_e^{-1} - 1)K_n$. These formulas are the same as those of Kozlov *et. al.* [3] except that they omitted the minus signs. A few other minor errors in their derivation are also corrected here. We note that $\gamma = C_P/C_v$ is the specific heat ratio, α_u and α_e are the accommodation coefficients, both of which are assumed to have a value of 0.9, and K_n is the (dimensionless) Knudsen number given by $K_n = \lambda/a$, where $\lambda = 60$ nm is the molecular mean free path. Substituting

$$\tilde{u}(w) = -\frac{1}{i\omega\rho_0}\frac{\partial\tilde{p}}{\partial z}\left(1 - F(k_V, w, B_u)\right), \qquad (18)$$

$$\tilde{\tau}(w) = \frac{\tilde{p}}{\rho_0 C_P}\left(1 - F(k_T, w, B_e)\right) \qquad (19)$$

in Eqs. (11) and (15) respectively leads to a new pair of equations

$$(\nabla^2 + k_V^2)F(k_V, w, B_u) = 0, \qquad (20)$$

$$(\nabla^2 + k_T^2)F(k_T, w, B_e) = 0, \qquad (21)$$

where $k_T = \sqrt{P_r}k_V$. Eqs. (20) and (21) are subject to the boundary conditions

$$F(k_V, a, B_u) + aB_u\frac{\partial}{\partial w}F(k_V, w, B_u)\Big|_{w=a} = 1, \qquad (22)$$

$$F(k_T, a, B_e) + aB_e\frac{\partial}{\partial w}F(k_T, w, B_e)\Big|_{w=a} = 1 \qquad (23)$$

Solutions to Eqs. (20) and (21) are given by

$$F(k_V, w, B_u) = AJ_0(k_V w), \qquad (24)$$

$$F(k_T, w, B_e) = BJ_0(k_T w). \qquad (25)$$

The unknown coefficients can be found by substituting Eqs. (24) and (25) in the boundary conditions of Eqs. (22) and (23) respectively to give $A = \left(J_0(k_V a) - B_u k_V a J_1(k_V a)\right)^{-1}$ and $B = \left(J_0(k_T a) - B_e k_T a J_1(k_T a)\right)^{-1}$. The average values across the tube cross-section are defined by

$$\begin{aligned}\left\langle F(k_V, a, B_u)\right\rangle &= \frac{1}{\pi a^2}\int_0^{2\pi}\int_0^a F(k_V, w, B_u)w\,dw\,d\phi \\ &= \frac{Q(k_V a)}{1 - 0.5B_u k_V^2 a^2 Q(k_V a)},\end{aligned} \qquad (26)$$

where $Q(x) = 2J_1(x)/(xJ_0(x))$ and similarly

$$\left\langle F(k_T, a, B_e)\right\rangle = \frac{Q(k_T a)}{1 - 0.5B_e k_T^2 a^2 Q(k_T a)}. \qquad (27)$$

3.5 Mass conservation and Helmholtz wave equation

Finally, we use the following mass conservation equation or equation of continuity [5]

$$i\omega\left(\left\langle\tilde{\delta}\right\rangle + \left\langle\tilde{\delta}_a\right\rangle\right) + \rho_0\frac{\partial}{\partial z}\left\langle\tilde{u}\right\rangle = 0. \qquad (28)$$

For the average velocity, we can write from Eq. (18)

$$\left\langle\tilde{u}\right\rangle = -\frac{1}{i\omega\rho_0}\frac{\partial\tilde{p}}{\partial z}\left(1 - \left\langle F(k_V, a, B_u)\right\rangle\right). \qquad (29)$$

Differentiating Eq. (29) with respect to *z* and inserting it in Eq. (28) yields

$$\left\langle\tilde{\delta}\right\rangle = -\frac{1}{\omega^2}\left(1 - \left\langle F(k_V, a, B_u)\right\rangle\right)\frac{\partial^2\tilde{p}}{\partial z^2} - \left\langle\tilde{\delta}_a\right\rangle, \qquad (30)$$

where $\tilde{\delta}_a$ is given by Eq. (9). Also, from the gas law of Eq. (12)

$$\frac{\tilde{p}}{P_0} = \frac{\left\langle\tilde{\delta}\right\rangle}{\rho_0} + \frac{\left\langle\tilde{\tau}\right\rangle}{T_0}, \qquad (31)$$

where the average temperature is derived from Eq. (19) as follows

$$\left\langle\tilde{\tau}\right\rangle = \frac{\tilde{p}}{\rho_0 C_P}\left(1 - \left\langle F(k_T, a, B_e)\right\rangle\right) \qquad (32)$$

Substituting Eq. (32) in Eq. (31) while noting that $C_P - C_v = P_0/(\rho_0 T_0)$ and $\gamma = C_P/C_v$ gives

$$\left\langle\tilde{\delta}\right\rangle = \frac{\rho_0}{\gamma P_0}\left(1 + (\gamma - 1)\left\langle F(k_T, a, B_e)\right\rangle\right)\tilde{p}. \qquad (33)$$

Equating Eqs. (30) and (33) then leads to the following Helmholtz wave equation

$$\frac{\partial^2\tilde{p}}{\partial z^2} + k^2\tilde{p} = 0, \qquad (34)$$

where

$$\begin{aligned}k^2 &= \frac{\omega^2\rho_0}{\left(1 - \left\langle F(k_V, a, B_u)\right\rangle\right)\gamma P_0} \\ &\times\left(1 + (\gamma - 1)\left\langle F(k_T, a, B_e)\right\rangle + \frac{\gamma P_0 k_a k_d \rho_N}{(i\omega + \omega_a)\omega_a\rho_0}\right).\end{aligned} \qquad (35)$$

3.6 Dynamic density

In order to simplify the wave number, we can use the following shorthand known as the dynamic density where $\left\langle\tilde{u}\right\rangle$ is given by Eq. (29) so that

$$\begin{aligned}\rho &= -\frac{1}{i\omega\left\langle\tilde{u}\right\rangle}\frac{\partial\tilde{p}}{\partial z} = \frac{\rho_0}{1 - \left\langle F(k_V, a, B_u)\right\rangle} \\ &= \rho_0\left(1 - \frac{Q(k_V a)}{1 - 0.5B_u k_V^2 a^2 Q(k_V a)}\right)^{-1}.\end{aligned} \qquad (36)$$

3.7 Dynamic compressibility

Also, the dynamic compressibility is defined by

$$C = \frac{\left\langle\tilde{\delta} + \tilde{\delta}_a\right\rangle}{\rho_0\tilde{p}}. \qquad (37)$$

From the ideal gas law of Eq. (33) we obtain

$$\frac{\left\langle\tilde{\delta}\right\rangle}{\rho_0\tilde{p}} = \frac{1}{\gamma P_0}\left(1 + (\gamma - 1)\left\langle F(k_T, a, B_e)\right\rangle\right), \qquad (38)$$

which, together with Eq. (9), is inserted in Eq. (37) to give

$$C = \frac{1}{\gamma P_0}\left(1 + \frac{(\gamma - 1)Q(k_T a)}{1 - 0.5B_e k_T^2 a^2 Q(k_T a)} + \frac{\gamma P_0 k_a k_d \rho_N}{(i\omega + \omega_a)\omega_a\rho_0}\right), \qquad (39)$$

so that the wave number simply becomes

$$k = \omega\sqrt{\rho C} \qquad (40)$$

and the characteristic specific impedance of an infinite tube is

$$Z_0 = \sqrt{\rho / C}. \qquad (41)$$

4 Finite blocked tube model

The solution to Eq. (34) is of the form

$$\tilde{p}(z) = \tilde{A}e^{ikz} + \tilde{B}e^{-ikz}, \qquad (42)$$

where z is the distance along the axis of the tube. From Eq. (36) the velocity is given by

$$\langle \tilde{u}(z) \rangle = -\frac{1}{i\omega\rho}\frac{\partial}{\partial z}\tilde{p}(z) = -\frac{k}{\omega\rho}(\tilde{A}e^{ikz} - \tilde{B}e^{-ikz}). \quad (43)$$

If the tube is blocked at $z = 0$, then $\langle \tilde{u}(0) \rangle = 0$ so that $\tilde{B} = \tilde{A}$. Also, if there is a piston at $z = h$ with velocity $\tilde{u}_0$, then $\langle \tilde{u}(h) \rangle = -(2ik\tilde{A}\sin kh)/(\omega\rho) = \tilde{u}_0$ so that

$$\tilde{A} = -\frac{\omega\rho\tilde{u}_0}{2ik\sin kh}. \quad (44)$$

This means that at $z = h$ the pressure becomes

$$\tilde{p}(h) = -\frac{\omega\rho}{ik}\tilde{u}_0 \cot kh. \quad (45)$$

Hence the specific acoustic input impedance at the piston is

$$Z_I = -\frac{\tilde{p}(h)}{\tilde{u}_0} = \frac{\omega\rho}{ik}\cot kh = -iZ_0 \cot kh. \quad (46)$$

5 Short-Tube/Large-wavelength model

The viscous boundary layer thickness is defined by

$$\delta_{visc} = \sqrt{\mu/(\omega\rho_0)}. \quad (47)$$

Hence the frequency at (and below) which the boundary layer occupies the whole cross-section of the tube is given by

$$\omega_{BL} = \mu/(\rho_0 a^2). \quad (48)$$

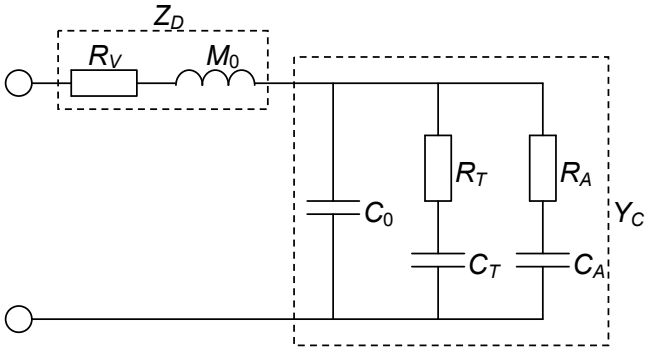

Figure 2. Blocked tube equivalent electrical circuit

At low frequencies, a closed tube can be modeled using the equivalent electrical circuit shown in Figure 2 where

$$C_0 = h/(\gamma P_0), \quad (49)$$

$$C_T = (\gamma - 1)C_0, \quad (50)$$

$$R_T = \frac{(1+4B_e)P_r}{8\omega_{BL}C_T} = \frac{(1+4B_e)\gamma P_0 a^2}{8(\gamma-1)\kappa T_0 C_T}, \quad (51)$$

$$C_A = \frac{P_0 k_a k_d \rho_N}{\omega_a^2 \rho_0}C_0, \quad (52)$$

$$R_A = 1/(\omega_a C_A), \quad (53)$$

$$M_0 = \rho_0 h/2, \quad (54)$$

$$R_V = \frac{16\omega_{BL}M_0}{3(1+4B_u)} = \frac{8\mu h}{3(1+4B_u)a^2}. \quad (55)$$

At low frequencies

$$Z_I \approx Z_D + Y_C^{-1}, \quad (56)$$

where the dynamic density impedance Z_D is given by

$$Z_D = R_V + i\omega M_0 \quad (57)$$

and the dynamic compressibility admittance Y_C is given by

$$Y_C = i\omega C_0 + \left(R_T + \frac{1}{i\omega C_T}\right)^{-1} + \left(R_A + \frac{1}{i\omega C_A}\right)^{-1}. \quad (58)$$

However, if $\omega_{BL} > 10\omega_T$, then for $\omega > 2\omega_T$, cot $kh \to 1$ and we have

$$Z_I \approx \sqrt{\frac{8Z_D}{3Y_C}}, \quad (59)$$

where ω_T is the transition frequency at which $Z_D Y_C = 1$ and above which $Z_D Y_C > 1$. These values are for the specific impedance, which is the ratio of pressure to particle velocity at the mouth. The capacitor C_0 represents the compliance of the tube assuming adiabatic pressure fluctuations without any thermal conduction or adsorption/desorption. The capacitor C_T represents the increase due to thermal conduction so that (C_0 + C_T) represents the total compliance assuming isothermal pressure fluctuations. In series with C_T is a resistor R_T representing the energy loss due to heat conduction through the wall. The capacitor C_A represents the compliance due to adsorption and desorption. In series with it is a notional resistor R_A representing the energy loss due to the adsorption/desorption relaxation time. The upper frequency limit f_U at which adsorption is effective is

$$f_U = \frac{1}{2\pi R C_A} = \frac{\omega_a}{2\pi} = \frac{k_a P_0 + k_d}{2\pi}. \quad (60)$$

It can be seen that the compliance C_A is maximum when $k_d = k_a P_0$ and $\rho_N >> \rho_0$. The ratio ρ_N / ρ_0 is inversely proportional to the tube diameter. For a hexagonal array of holes, the fill factor, which is the ratio of the area covered by the holes to the total area, is given by

$$fill\_factor = \frac{2\pi \times radius^2}{\sqrt{3} \times hole\_pitch^2}. \quad (61)$$

The specific impedance of such an array is then the impedance at the mouth each tube divided by the fill factor, as plotted in Figure 3 and Figure 4.

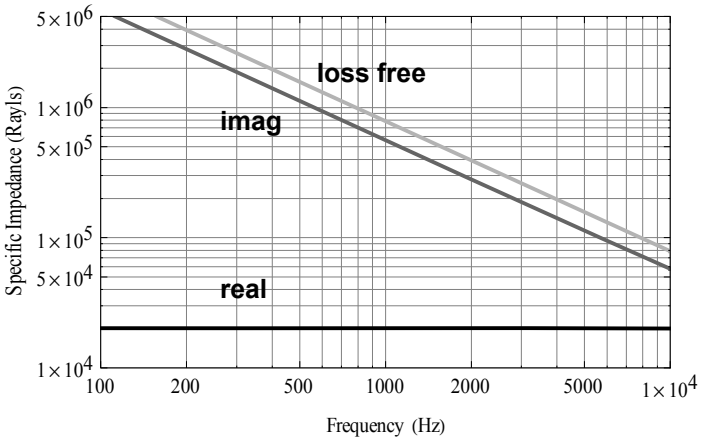

Figure 3. Specific acoustic impedance of array of tubes without adsorption, where a = 1 μm and h = 0.25 mm. Fill factor is 22.7 %.

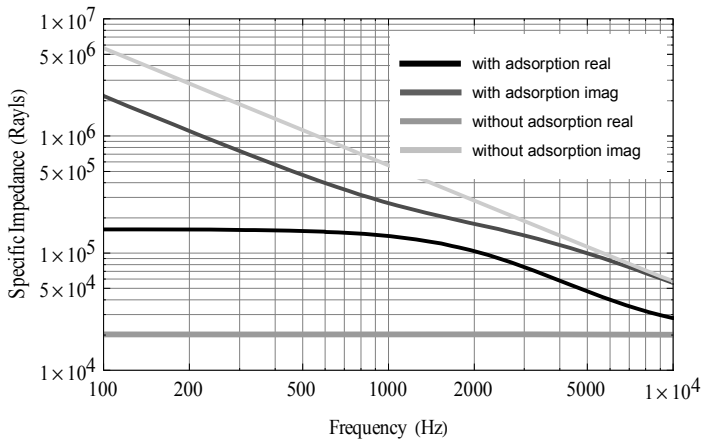

Figure 4. Specific acoustic impedance of array of tubes with and without adsorption, where a = 1 μm, h = 0.25 mm, k_a = 0.03 and k_d = 3000. Fill factor is 22.7 %.

6 The etching process

Deep reactive ion etching (DRIE) using the BOSCH process allows the production of high aspect ratio structures in crystalline silicon wafers [6]. This is achieved by using a cyclical etching process. The areas of the sample that are not to be etched are protected by a layer of photoresist or other hard masking material (such as silicon dioxide). The sample is then loaded into a vacuum system and exposed to a dense plasma of SF_6 gas. The SF_6 plasma etches the exposed silicon very effectively, but also starts to undercut the masked area as shown in Figure 5. Therefore, after a few seconds, the SF_6 plasma is replaced by a C_4F_8 plasma, which coats the exposed silicon in a thin polymer layer. After a few more seconds, the C_4F_8 plasma is replaced by the SF_6 plasma once more. The SF_6 plasma removes the protective polymer coating from the bottom of any exposed areas more quickly than on the side-walls, and so the etch only proceeds downwards. Therefore, by cycling these two plasmas, high aspect ratio structures may be produced in the silicon wafer, such as the micro-holes required in this work.

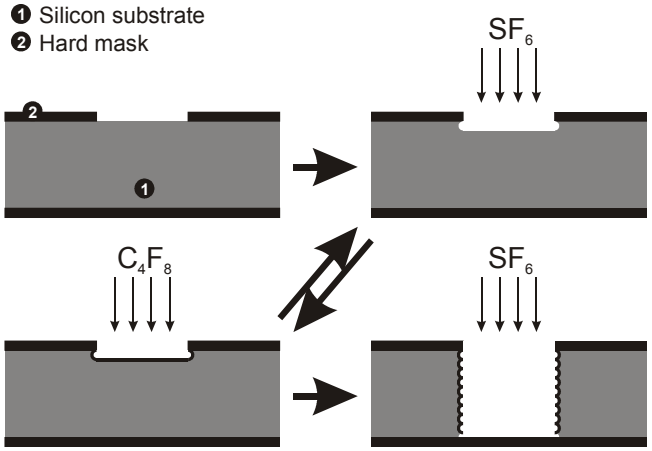

Figure 5. Schemetic diagram of the deep reactive ion etching process.

7 Measurements

Unfortunately, no results were available by the submission deadline for this paper at which time the maximum etch depth obtained was 60 μm before the photoresist finally expired. However, it is anticipated that with some improved etching techniques, measurements will be available by the time of the presentation. These will be made in a free field using a velocity transducer known as a "microflown" [7] in proximity to the duct openings in order to measure the particle velocity. A conventional pressure microphone will also be used in order to calculate the pressure to particle velocity ratio and hence specific acoustic impedance.

8 Discussion and conclusion

In the absence of measured results, the adsorption/desorption relaxation coefficients k_a, k_d and the area S_m occupied by each adsorbed molecule have been "guesstimated" for the simulation shown in Figure 4. In Figure 3, without adsorption, the imaginary impedance is reduced by a factor of $1/\gamma$ due to thermal conduction alone. In Figure 4, a greater reduction can be seen due to adsorption. In order to achieve a high cut-off frequency, it is desirable for k_a and k_d to be as large as possible and ideally $k_d \approx k_a P_0$ in order to maximize the compliance. These are dependent upon the adsorbing material used together with its lattice structure. Also, the compliance increases with the adsorption capacity ρ_N, which is proportional to the adsorption surface area and is thus a function of the tube diameter as well as depending upon S_m, which is a material property. More experimental work needs to be done to determine the values of these parameters for other materials.

References

[1] J. R. Wright, "The virtual loudspeaker cabinet," *J. Audio Eng. Soc.* **51**(4), 244-247 (2003).

[2] F. Bechwati, O. Umnova, T. Cox, "New semi-empirical model for sound propagation in absorbing microporous solids (activated carbon)," on the CD ROM: *19th International Congress on Acoustics Madrid*, 2-7 September 2007

[3] V. F. Kozlov, A. V. Fedorov, "Acoustic properties of rarefied gases inside pores of simple geometries," *J. Acoust. Soc. Am.* **117**(6), 3402-3412 (2005).

[4] Timo Veijola, "A two-port model for wave propagation along a long circular microchannel," *Microfluidics and Nanofluidics*," **3**(3), 359-368 (2007).

[5] P. M. Morse, K. U. Ingard, *Theoretical Acoustics,* McGraw-Hill, New York (1968), pp. 239, 279, 281.

[6] A. A. Ayon, R. L. Bayt, K. S. Breuer, "Deep reactive ion etching: a promising technology for micro- and nanosatellites," *Smart Materials & Structures*, 10, pp. 1135-1144 (2001).

[7] Finn Jacobsen, Hans-Elias de Bree, "A comparison of two different sound intensity measurement principles," *J. Acoust. Soc. Am.* **118**(3), 1510-1517 (2005)